iScience

CellPress
OPEN ACCESS

Article

Decoding human spontaneous spiking activity in medial temporal lobe from scalp EEG

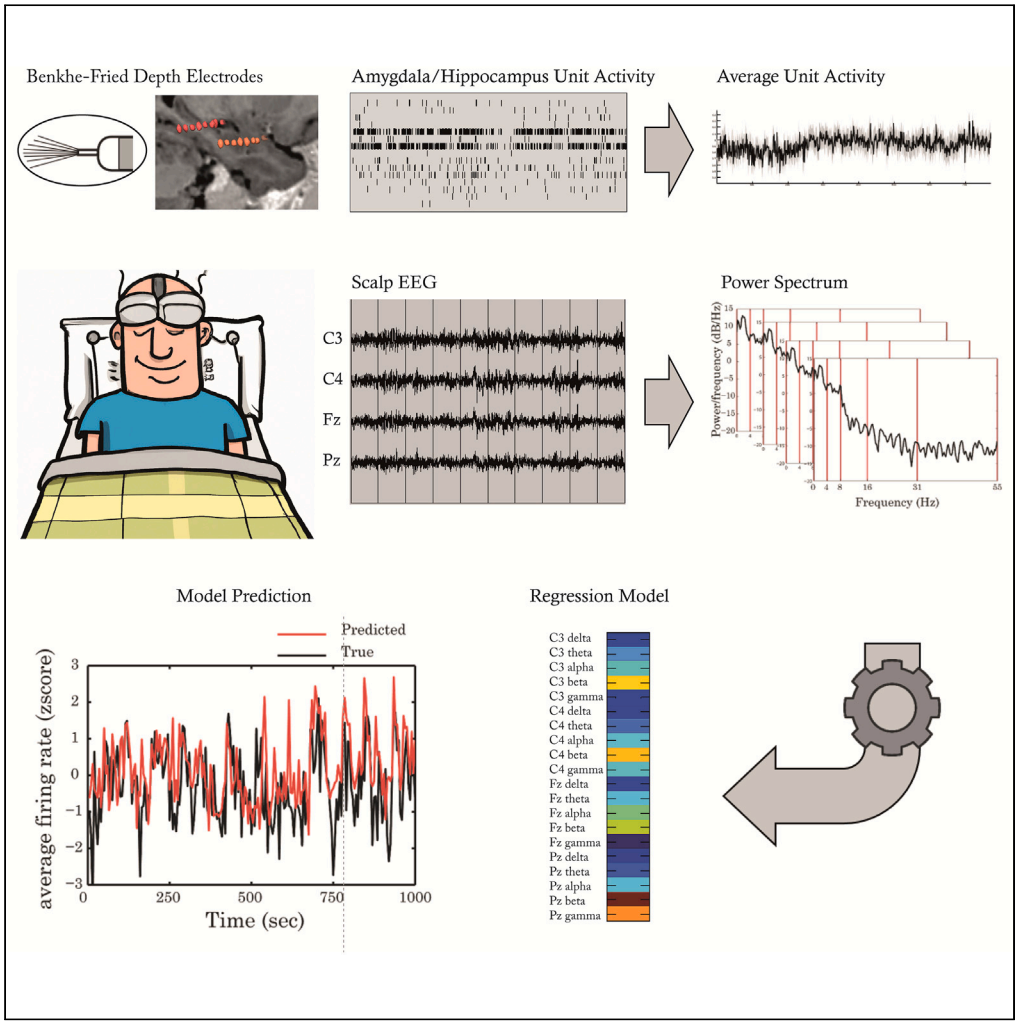

Hagar G. Yamin, Guy Gurevitch, Tomer Gazit, ..., Yuval Nir, Yoav Benjamini, Talma Hendler

hendlert@gmail.com

Highlights

Scalp EEG features predicted human MTL spiking activity during sleep and wakefulness

Regional specificity was found for amygdala and hippocampus models

Prediction accuracy emerges from short- and long-term fluctuations in firing rates

Yamin et al., iScience 26, 106391
April 21, 2023 © 2023 The Authors.
https://doi.org/10.1016/j.isci.2023.106391

iScience

CellPress
OPEN ACCESS

Article

Decoding human spontaneous spiking activity in medial temporal lobe from scalp EEG

Hagar G. Yamin,[1] Guy Gurevitch,[1,2] Tomer Gazit,[1,2] Lavi Shpigelman,[3] Itzhak Fried,[2,4,5] Yuval Nir,[2,6,9,10,11] Yoav Benjamini,[6,7,11] and Talma Hendler[1,2,6,8,11,12,*]

SUMMARY

Linking scalp electroencephalography (EEG) signals and spontaneous firing activity from deep nuclei in humans is not trivial. To examine this, we analyzed simultaneous recordings of scalp EEG and unit activity in deeply located sites recorded overnight from patients undergoing pre-surgical invasive monitoring. We focused on modeling the within-subject average unit activity of two medial temporal lobe areas: amygdala and hippocampus. Linear regression model correlates the units' average firing activity to spectral features extracted from the EEG during wakefulness or non-REM sleep. We show that changes in mean firing activity in both areas and states can be estimated from EEG (Pearson r > 0.2, $p \ll 0.001$). Region specificity was shown with respect to other areas. Both short- and long-term fluctuations in firing rates contributed to the model accuracy. This demonstrates that scalp EEG frequency modulations can predict changes in neuronal firing rates, opening a new horizon for non-invasive neurological and psychiatric interventions.

INTRODUCTION

Non-invasive tracking of electrophysiological patterns deriving from neurons located in deep brain regions encompasses the potential of being a game changer in neuropsychiatry. Such ability could serve the development of biomarkers, as well as identification of targets for neuromodulation. However, this desired goal is hampered by two main limitations of scalp electroencephalography (EEG), the most common non-invasive electrophysiological recording technique.

First, a leading assumption is that scalp EEG, like intracranial field potentials, originate primarily from post-synaptic activity arising in the apical dendrites of pyramidal cortical cells and less so from single neurons' action potentials.[1,2] Second, neural activity of deeply located regions such as in the mesial temporal lobe (MTL), have been regarded as undetectable on the scalp due to the rapid decay of the EEG signal from deeper brain sources and due to the cellular architecture of these structures that have been considered as closed-field.[3] This assumption has been recently challenged by statistical methods used to depict amygdala activity marked by fMRI.[4,5] Yet the consensus remains that currents reaching the scalp from deep brain areas would be very weak, particularly from the high frequency bands which are most correlated with unit activity[6,7] and whose power decays most rapidly with distance.[8]

This paper presents the results from a data science study using human simultaneous recording of single unit spiking activity in MTL and scalp EEG in order to obtain a prediction model for localized intracranial neural activity.

Major MTL structures such as the amygdala and hippocampus are thought to play a central role in various cognitive processes that underlie neuropsychiatric disturbances including memory, emotion, and motivation. In psychiatry, accumulating evidence from animal models and neuroimaging studies in humans show that hyperactive amygdala could be predictive of post-traumatic stress disorder (PTSD) development following exposure to potentially traumatic stress.[9–12] Amygdala abnormality; however, is transdiagnostic as evident from neuroimaging studies in anxiety, depression, and personality disorders.[13] Similarly, animal models demonstrated alterations in amygdala single cell activity related to anxiety[14,15] and schizophrenia-like syndrome.[16] The hippocampus seems critical for adaptive encoding and consolidation of the traumatic memory, thus could mediate recovery from trauma and effectiveness of therapeutic effort.[10,11] Reduced hippocampal volume in individuals with PTSD has been repeatedly observed along with post-traumatic

[1]Sagol Brain Institute, Wohl Institute for Advanced Imaging, Tel-Aviv Sourasky Medical Center, Tel-Aviv 6423906, Israel

[2]Department of Physiology & Pharmacology, Sackler School of Medicine, Tel-Aviv University, Tel-Aviv 6997801, Israel

[3]IBM Research, Haifa 3498825, Israel

[4]Department of Psychiatry and Biobehavioral Sciences, Jane and Terry Semel Institute for Neuroscience and Human Behavior, University of California Los Angeles, Los Angeles, CA 90024, USA

[5]Department of Neurosurgery, David Geffen School of Medicine, University of California Los Angeles, Los Angeles, CA 90095, USA

[6]Sagol School of Neuroscience, Tel-Aviv University, Tel-Aviv 6997801, Israel

[7]Department of Statistics and Operations Research, Tel-Aviv University, Tel-Aviv 6997801, Israel

[8]School of Psychological Sciences, Faculty of Social Sciences, Tel-Aviv University, Tel-Aviv 6997801, Israel

[9]Department of Biomedical Engineering, Faculty of Engineering, Tel Aviv University, Tel Aviv 6997801, Israel

[10]The Sieratzki-Sagol Center for Sleep Medicine, Tel Aviv Sourasky Medical Center, Tel Aviv 6423906, Israel

[11]These authors contributed equally

[12]Lead contact

*Correspondence: hendlert@gmail.com

https://doi.org/10.1016/j.isci.2023.106391

This is an open access article under the CC BY-NC-ND license (http://creativecommons.org/licenses/by-nc-nd/4.0/).

molecular changes including decreased brain-derived neurotrophic factor (BDNF), impaired neurogenesis in the dentate gyrus, decreased long-term potentiation in the CA1 region, and dendritic retraction in CA3.[17] MTL also constitute an important source of abnormal neural activity in epilepsy. Temporal lobe epilepsy (TLE) is the most common form of epilepsy with focal seizures and in many cases originates from the amygdala and/or hippocampus. Lastly, animal work repeatedly showed abnormal activity in hippocampal neurons in Alzheimer's disease models.[18] Altogether this evidence emphasize that non-invasive yet reliable recording of activity arriving from the amygdala and hippocampus could be of special value for advancing mechanism-driven diagnosis and intervention strategies in psychiatry and neurology.[19]

Tracking patterns of neuronal activity in deep brain structures using scalp EEG could be possible indirectly, given that some cortical regions that are closer to the scalp may show correlated activity with deep regions of interest during shared state changes. Both the amygdala and hippocampus have numerous connections to cortical structures, from sensory areas to the pre-frontal cortex, forming cortical-limbic dynamical networks.[9,20] Thus, by simultaneously tracking cortical and MTL subcortical structures it could be possible to detect correlates of deep brain activity using non-invasive measures. In a previous study, we showed that using machine learning it is possible to obtain an EEG model informed by amygdala fMRI BOLD activation (termed electrical finger print, EFP).[21] The amygdala-EFP model was validated by showing its correspondence with amygdala BOLD modulation via fMRI performed on a new group[19] and by employing it in neurofeedback to improve stress resilience among soldiers.[22] Nevertheless, using simultaneous scalp EEG recording in the MRI scanner as the source for the amygdala-EFP inevitably introduces noise to the model due to the nature of BOLD being an indirect measure of neural activity and the introduction of MRI induced artifacts to the EEG signal.

Aspiring to establish a more direct estimation of MTL activity from EEG, in this study we used simultaneous neuronal spiking activity from intracranial contacts located in the amygdala and hippocampus, together with EEG from four scalp electrodes obtained from six individuals with intractable epilepsy acquired overnight during periods of wakefulness and non-rapid eye movement (NREM) sleep (402.94 $\pm$ 11.70 min, mean $\pm$ sem). We used unit recordings from contacts in the pre-frontal cortex as a control region outside the MTL. To deal with the complex relation between spiking activity and EEG spectral information, we applied a statistical approach by means of linear regression using the power in the traditional EEG bands as predictors of the average unit activity. In light of recent findings correlating scalp activity with deep brain sources,[5] we hypothesized that this analysis will result in significant and unique prediction of unit spike activity per region from simultaneous scalp EEG recording.

RESULTS

Estimating mean firing rates from EEG is region specific

Neuronal firing rates (FR) in the amygdala and hippocampus were modeled from scalp EEG in 5s bins within-subject using 5-fold cross-validation. We split the data into five consecutive non-overlapping segments, training the model over 4/5 segments and testing for accuracy on the remaining segment. Owing to the variation in spectral properties between wakefulness and NREM sleep,[23] we modeled each state separately (see STAR Methods). Pearson correlation coefficient and in some cases root mean squared error (RMSE) between true and predicted FR were calculated as performance measures.

Figure 1A depicts test versus train RMSE prediction error, constituting the objective function of the linear model. As expected, the range of the train RMSE was smaller than that of the test (i.e., better fit), and in most cases it was lower than the test error. There were no major differences in model performance (RMSE) across different subjects, areas or brain states.

Figure 1B shows an example of the hippocampal model's performance for one patient during NREM sleep where the correlation coefficient ($r = 0.4$) was calculated by sequentially concatenating all test segments.

Test correlations for each model were calculated for the area for which the model was developed (amygdala or hippocampus), and in order to assess the regional specificity of the model, we used the model to predict the firing rate in two other areas (amygdala or hippocampus and frontal cortex, FC). Test correlations for all six patients in each brain area and state are summarized in Figures 1C–1F. All regression models are significant (F-test, $p \ll 0.001$, see STAR Methods), and the majority (18/24 models, one-sided binomial test, $p = 0.02$) of the test correlations are within the range of 0.2–0.6, depicting a weak to moderate positive correlation. Correlation values were also tested for significance with a one-sided test and a p value of 0.01

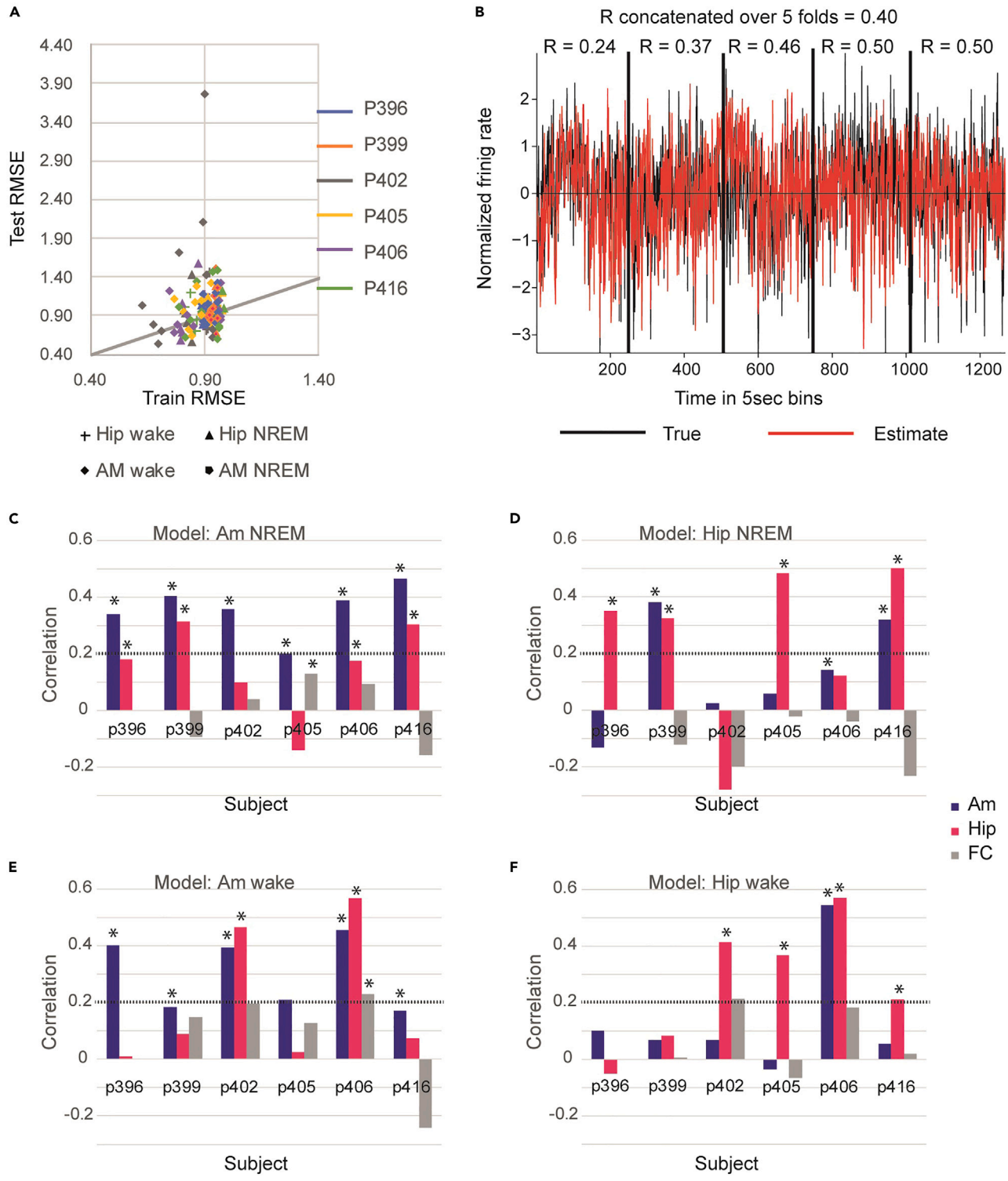

Figure 1. MTL average unit activity can be estimated using features extracted from the EEG

(A) Test vs. train RMSE per fold. Each color represents a different subject and each shape represents a region and state (see legend). The train and test RMSE are similar across subjects, regions, and states. As expected, the train accuracy is less variable and usually better than that of the test.

Figure 1. *Continued*

(B) An example of a 5-fold prediction from the amygdala of one subject (P399) during non-REM sleep. The black trace represents a true firing rate after transformation (see STAR Methods), and the red trace represents the model prediction. Each vertical line is a transition point between each test period. Above each section the true to prediction correlation is noted, and the total test correlation overall test periods concatenated to each other equals to 0.4. (C–F) Test correlations for the target area (amygdala or hippocampus) and for the two other areas (Am or Hipp and FC) for each area and state. Significant test correlations are noted with * ($p < 0.01$, bonferroni corrected). The dashed line marks a non-negligible correlation value of 0.2. For most models, the highest test correlation is with the target area of the model.

(Bonferroni corrected for all the different models; n = 68). In most cases (15/18 models) where a non-negligible correlation was found with the target area (higher than 0.2), the model accuracy of the target area was the highest than the two other areas. When the correlation was highest in a brain region other than the target, it was found within the MTL (amygdala or hippocampus) and never within the FC. Examining the correlation between amygdala and hippocampus firing rate revealed high and significant correlations in those cases (see Figure S1). Rare cases of high correlations may be attributed to the functional relationship between the amygdala and hippocampus.[24]

Model coefficients for non-rapid eye movement sleep are more stable than awake signals

To evaluate the similarity between the models' coefficients across the different folds, we calculated the mean euclidean distance between coefficients of all possible pairs of models for the same patient, region, and state. We observed that NREM sleep models were more stable than wakefulness models (signed-rank test: N = 12, W = 10, Z = 2.27, p = 0.02) (Figure 2A). 10 of the 12 models showed a larger variation in model coefficients within the wakefulness state than NREM sleep.

Finally, a full model was fit for each patient, region, and state using all available data (all 5 time-sections). The amplitudes of the specific coefficients of these models were variable, and the low number of subjects prevents drawing statistical conclusions (Figure S4). Nevertheless, when focusing on NREM sleep (a state of higher model stability) and on patients in which models performed well (with a mean correlation above 0.2), we observed relatively high beta band coefficients in both amygdala and hippocampus models (Figures 2B and 2C).

Prediction's accuracy emerges from both short- and long-term fluctuations in firing rates

Figures 3A–3D features single patient examples of model predictions for the amygdala and hippocampus in either wakefulness or NREM sleep using the entire dataset (full model). We verified that the measured correlation does not benefit from adding the firing rate in frontal areas or arousal, by creating two additional models, which include an estimate of FC activity or a proxy of arousal measured by an estimate of the 1/f slope in the frequency band 30–45 Hz[25] (see STAR Methods). In the combined models, model accuracy as measured by the adjusted R^2 values does not improve by adding the additional features. (Figure S5). To make sure these additional features are not by themselves explanatory of MTL firing rate, we also show that predictions based solely on these features are much worse than the original models (Figure S5).

The measured correlations could arise from momentary changes in firing rates, from long-term changes in firing rates, or from a combination of both. Long-term changes in firing rate could be attributed to state transitions in the entire network. Though both short- and long-term fluctuations are of importance, we sought to validate whether the model's prediction can be attributed to one over the other. In order to do so, we created for each patient, region and state separately, a series of models predicting shifted MTL FR from unshifted scalp EEG (5– 300 s shifts, see STAR Methods). If such short time shifts would cause a decrease in model prediction, it would support the notion that the model does not only take into account long-term fluctuations.

In 18/24 models correlation decayed rapidly with time shifts (in the shortest 5 s shift) indicating that a significant part of the model correlation is due to short time dependencies (Figure S6). Figures 3E–3H summarize the results of evaluating the model's prediction compared to the distribution of the shifted models. During wakefulness, the accuracy of the unshifted model's prediction was in the region where it was identified as an outlier relative to the distribution of the shifted models in 10 out of the 12 models (five out of six models in both tested regions). During NREM sleep, it occurred for five (out of six) subjects for the amygdala and in four (out of six) for the hippocampus. For both states, the unshifted correlation was the extreme data point in 17 models. Thus, in 70% (17/24) of the cases (95% CI: 52%–100%) the correlations arise from short time dependencies and not only due to long-term changes in firing rates.

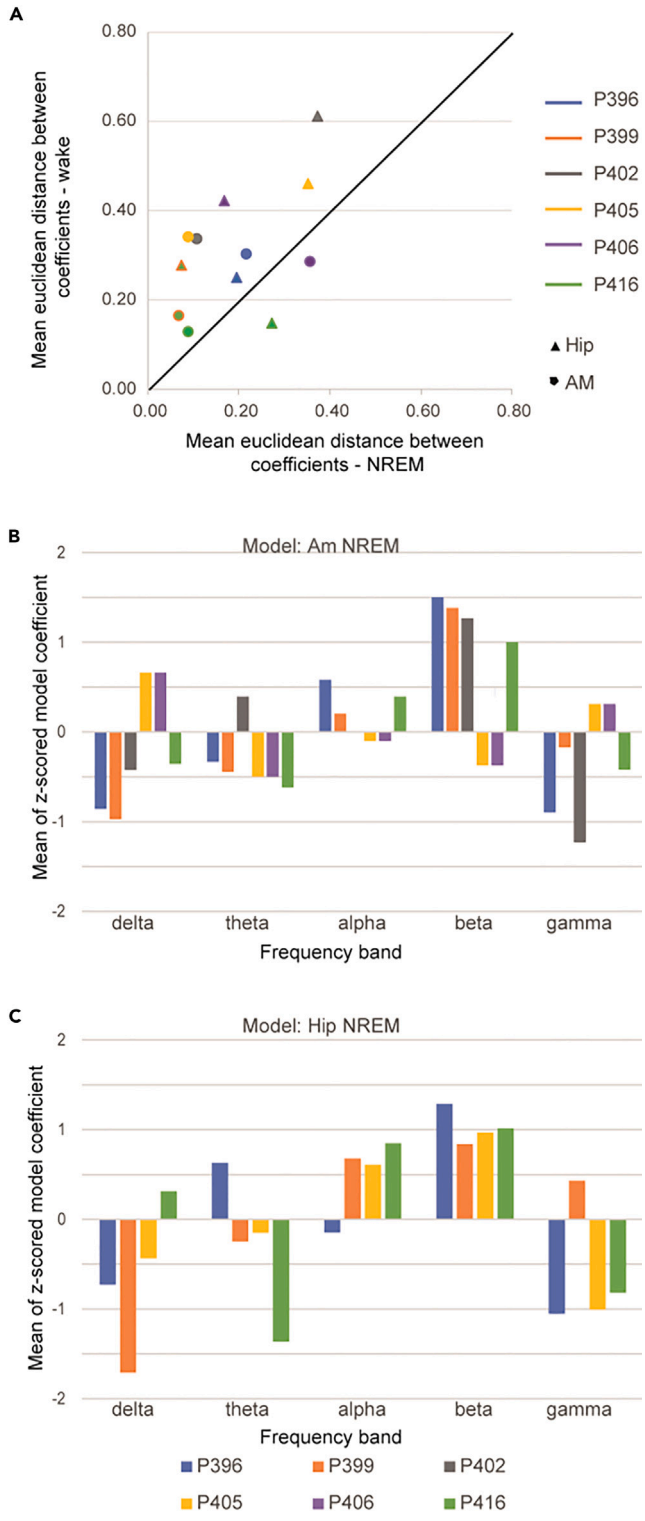

Figure 2. Model stability and coefficients

(A) Mean euclidean distance between the coefficients of the different models (folds) for the awake vs. NRS period. Dots represent region/patient. Dot location above the diagonal line represents higher coefficient stability for NRS than wake period. (B and C) Mean coefficients for each frequency band of the successful models (i.e., correlation with signal > 0.2) in the full NRS amygdala (B) and hippocampus (C) models.

DISCUSSION

We demonstrate here the feasibility of estimating the dynamics of averaged neuronal spiking activity in human MTL using features extracted from simultaneously acquired scalp EEG. The model performance as measured by both RMSE and Pearson correlation was of similar range for the two regions used for unit recording; amygdala and hippocampus and for both states of wakefulness and NREM sleep (Figure 1). It was also demonstrated that the predictions are attributed to both short- and long-term changes in the firing rate and that they are regionally specific when each region is compared to unit activity in pre-frontal cortex and to the other MTL region (Figures 1 and 3). Altogether, these findings support the notion that tracking deep neural patterns in the MTL from scalp EEG recording is possible. These results do not imply that MTL currents are detected in scalp EEG, but rather that a statistical association is made possible indirectly by the abundant anatomical and functional connectivity between units in the amygdala and hippocampus and neural activity in the neocortex that is readily detected from the scalp EEG. As far as we know this is the first demonstration of limbic unit activity transformation from EEG; an affordable and accessible, non-invasive electrical recording technique. The demonstrated ability thus opens the potential usage of scalp EEG to guide monitoring or modulation of limbic MTL based activity. This is particularly appealing as the amygdala and hippocampus have been repeatedly indicated in several neuropsychiatric disorders.[10,17]

Several limitations of this work should be considered upfront. First, one should consider changes in the current flow over the scalp once the skull has been breached and electrodes are inserted. It may be claimed that scalp EEG recorded in this situation is not comparable to the EEG with an intact skull or once electrodes have been removed. However, previous reports either using Deep Brain Stimulation electrodes[5] or subdural electrodes[26] simultaneously with scalp EEG were able to show comparable source activity of the different frequency bands. We modeled the mean firing rate over multiple neurons in the amygdala or hippocampus in each individual; a relatively crude simplification of the complexity that entails the neural activity of a region. Obviously, each region encompasses multiple neuron types that differ in many dimensions such as their electrophysiological behavior, transmitters, and connectivity profiles. Second, each patient was implanted at slightly different locations and perhaps different sub-regions within the amygdala or hippocampus; both known to include multiple nuclei, sections, and cellular types.[27] Diverse neural firing patterns between the different sub-regions have been reported in both the amygdala and hippocampus.[14,28] Nevertheless, this work shows that despite this diversity, an average firing pattern in each monitored region can be modeled from the scalp of an individual, thus opening the path for utilizing EEG based reliable surrogates of deeply localized limbic neural activity.

What makes the intracranial-scalp transformation possible?

We suggest that the ability to depict deeply originated neuronal activity in MTL from non-invasive scalp EEG is made possible by a number of factors. First, harnessing the brain's ample connectivity and small world topography.[29] Both the amygdala and hippocampus have numerous connections to cortical structures, from sensory areas to the pre-frontal cortex, forming cortical-limbic/paralimbic dynamical networks.[30] Indeed it has been proposed that the amygdala's involvement in emotion regulation originates from its interactions with the cingulate cortex, orbitofrontal cortex, dorsolateral pre-frontal cortex, and the hippocampus.[31] In a similar manner, the hippocampus' involvement in memory formation and retrieval is associated with transient increases in cortico-hippocampal interactions including co-activation of the hippocampal with perirhinal, orbitofrontal, and posterior cingulate cortices.[32] An analogous scenario can be found in connectivity between basal ganglia and motor cortex circuits' in relation to movement processing. For example, Lalo et al.[33] found bidirectional coupling between scalp measured beta and gamma band EEG and intracranial field potentials recorded from depth electrodes in the subthalamic nucleus, and Gatev et al.[34] showed that unit activity in the extra-striatal basal ganglia is related to EEG oscillations measured from the scalp. It has also recently been shown that alpha oscillations generated in the thalamus and nucleus accumbens can be detected using source reconstruction of high-density scalp EEG.[5] Second, both rapid and slow changes in arousal, likely constitute a latent variable that affects both MTL firing rates and simultaneously recorded scalp EEG dynamics. For example, changes in sleep depth, as well as dynamics in vigilance and attention during wakefulness, likely contribute to the ability to relate intracranial MTL activity to scalp EEG when recorded simultaneously. During sleep specifically, higher slow wave activity is known to be associated with decreases in firing rates across most brain regions.[35]

Limitations of the study

Modeling neuronal firing using EEG recorded from the scalp is a promising approach allowing non-invasive monitoring of deeply originated neuronal activity. Yet, it is important to be aware of the limited framework

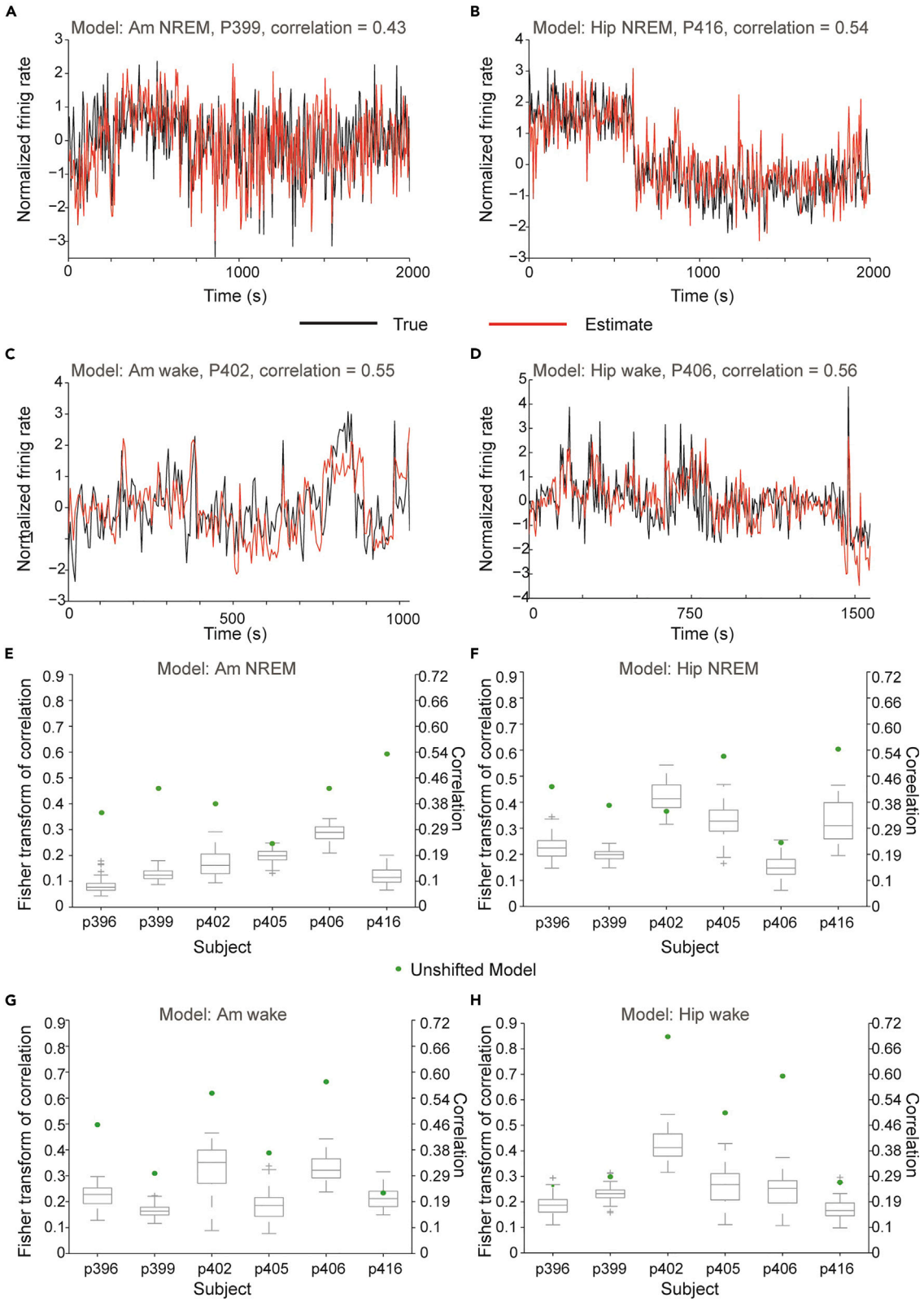
A
Model: Am NREM, P399, correlation = 0.43
Normalized frinig rate
Time (s)
B
Model: Hip NREM, P416, correlation = 0.54
Normalized frinig rate
Time (s)
True
Estimate
C
Model: Am wake, P402, correlation = 0.55
Normalized frinig rate
Time (s)
D
Model: Hip wake, P406, correlation = 0.56
Normalized frinig rate
Time (s)
E
Model: Am NREM
Fisher transform of correlation
Correlation
Subject
p396
p399
p402
p405
p406
p416
F
Model: Hip NREM
Fisher transform of correlation
Correlation
Subject
Unshifted Model
G
Model: Am wake
Fisher transform of correlation
Correlation
Subject
H
Model: Hip wake
Fisher transform of correlation
Correlation
Subject

Figure 3. Model accuracy can be attributed to both short- and long-term changes in firing rates

(A–D) True (black trace) vs. predicted (red trace) average unit activity after transformation (see STAR Methods) of the amygdala (A and C) from subjects p402 and p399, and hippocampus (B and D) from subjects p406 and p416 —during awake and non-REM sleep periods. The prediction is calculated using the train model without splitting to test and train periods. The overall correlation, which is stated in each graph, is composed from short- and long-term correlations.

(E–H) Fisher transform of the Pearson correlation between true and predicted firing rate for the amygdala (E and G) and hippocampus (F and H) during awake (E and F) and non-REM sleep (G and H) periods for the unshifted model (green dots) and boxplot of the fisher-transformed correlations for the shifted models (gray). Central mark indicates the median, and the bottom and top edges of the box indicate the 25th and 75th percentiles, respectively. The whiskers extend to the most extreme data point within 1.5 times the interquartile range; data points that are considered as potential outliers are marked in + sign. Note that in 19 of the 24 cases the correlation of the unshifted model is in the outlying region and in 17 of the 24 it is the most extreme point lying far away from the upper quartile. Indicating in these cases that the correlation can be attributed to short-term fluctuations in the firing rate. Right y axis indicates the untransformed Pearson's correlation values.

of the approach. In previous work by Whittingstall and Logothetis,[36] multi-unit activity from a monkey's visual cortex was modeled using scalp EEG while monkeys observed natural movies. Our current study follows their approach but with a more ambitious aim of modeling deeper limbic structures and without a provoking task in humans. Interestingly, model success as measured by the correlation between the predicted and true spike rate was similar in both studies ($r \sim = 0.2–0.3$). However, in their study the features best predicting neuronal firing rates were relatively stable over monkeys (i.e., gamma-band power, delta-band phase) whereas, we found large variability in the weighting of EEG features across models trained on the different subjects' data (Figures 2B and 2C). This inter-subject variability precludes development of a one-class generic model that can be used outside the realm of intracranial recording from each person (at least at present), largely hampering the scalability of the model's application in clinical setting. We further speculate that this difference between visual cortex and subcortical limbic models is due to different electrical and electrophysiological mechanisms of these areas. Since the visual cortex is closer to the scalp than the MTL, a more direct cortically based model can be obtained while an MTL model presumably relies on subcortical-cortical connectivity and latent variables, which could be more prone to between subject variability also in terms of momentary brain or mental state. In addition, since precise electrode locations were based on clinical needs, these data are inherently more variable between individuals than those animal studies. Additionally, specificity of this model to a certain region is inherently limited by the independency of the firing rate from other brain regions. We show that when frontal cortex units have highly correlated firing rates with amygdala/hippocampal units, the specificity of the model decreases. Future studies can pre-select periods of independent regional activity for a more specific modeling process.

In recent studies, we showed that an EEG based model of amygdala fMRI activation can be achieved.[19,21] While both our previous and current analyses try to model deep brain activity from scalp EEG they differ in the probe they try to model: BOLD amygdala activation in the previous work and amygdala or hippocampal neural activity in the current study. While BOLD fMRI is an indirect measure of neural activity, which depends on hemodynamic coupling, here we directly model neural activity *in situ*. In our previous work, we were able to produce a group EEG based model of amygdala fMRI activation. Due to the small number of subjects in the current work, we could not address model generalization over patients but rather present the robustness of per patient data. We hope that the increased usage of implanted electrodes and devices over the last decade, as well as the formation of international shared databases will allow similar analysis of larger datasets in the near future. General models will open the door to novel clinical applications ranging from online monitoring of disordered state biomarkers to closed loop non-invasive self-neuromodulation procedures (e.g., neurofeedback).

To sum, this work presents a novel modeling approach of neuronal firing rates in the human MTL through non-invasive scalp EEG, demonstrating the feasibility and location specificity of such approach. Further advancements and validations may prove this approach useful for clinical monitoring and targeted neuromodulation.

STAR★METHODS

Detailed methods are provided in the online version of this paper and include the following:

- KEY RESOURCES TABLE
- RESOURCE AVAILABILITY

SUPPLEMENTAL INFORMATION

Supplemental information can be found online at https://doi.org/10.1016/j.isci.2023.106391.

ACKNOWLEDGMENTS

We would like to thank Yuval Benjamini for assisting in the initial stages of data analysis. This work was partially funded by European Union Seventh Framework Program (FP7/2007–2013) under grant agreements no. 604102 (Human Brain Project, T.G. and T.H) and no. 294519 (PSARPS H.G.Y. and Y.B.), US National Science Foundation and U.S.-Israel Binational Science Foundation NSF-BSF grant 2017628 (I.F. & Y.N.), and ERC-2019-CoG 864353 (Y.N.).

AUTHOR CONTRIBUTIONS

Conceptualization: T.H., Y.N., I.F.; Methodology: H.G.Y., T.G., Y.B., L.S.; Investigation: H.G.Y., T.G., G.G., I.F.; Supervision: T.H., Y.B., Y.N.; Writing – original draft: H.G.Y., G.G., T.G.; Writing – review and editing: H.G.Y., G.G., T.G., T.H., Y.B., Y.N., I.F., and L.S.

DECLARATION OF INTERESTS

T.H. is an employee and shareholder of GrayMatters Health Ltd.

Received: December 1, 2021
Revised: June 16, 2022
Accepted: March 7, 2023
Published: March 11, 2023

REFERENCES

1. Nunez, P.L., and Srinivasan, R. (2006). Electric Fields of the Brain: The Neurophysics of EEG (Oxford University Press).

2. Logothetis, N.K. (2003). The underpinnings of the BOLD functional magnetic resonance imaging signal. J. Neurosci. *23*, 3963–3971. https://doi.org/10.1523/JNEUROSCI.23-10-03963.2003.

3. Hudry, J., Ryvlin, P., Royet, J.-P., and Mauguière, F. (2001). Odorants elicit evoked potentials in the human amygdala. Cereb. Cortex *11*, 619–627. https://doi.org/10.1093/cercor/11.7.619.

4. Attal, Y., Bhattacharjee, M., Yelnik, J., Cottereau, B., Lefevre, J., Okada, Y., Bardinet, E., Chupin, M., and Baillet, S. (2007). Modeling and detecting deep brain activity with MEG EEG. In 2007 29th Annual International Conference of the IEEE Engineering in Medicine and Biology Society, pp. 4937–4940. https://doi.org/10.1109/IEMBS.2007.4353448.

5. Seeber, M., Cantonas, L.-M., Hoevels, M., Sesia, T., Visser-Vandewalle, V., and Michel, C.M. (2019). Subcortical electrophysiological activity is detectable with high-density EEG source imaging. Nat. Commun. *10*, 753. https://doi.org/10.1038/s41467-019-08725-w.

6. Mazzoni, A., Whittingstall, K., Brunel, N., Logothetis, N.K., and Panzeri, S. (2010). Understanding the relationships between spike rate and delta/gamma frequency bands of LFPs and EEGs using a local cortical network model. Neuroimage *52*, 956–972. https://doi.org/10.1016/j.neuroimage.2009.12.040.

7. Nir, Y., Fisch, L., Mukamel, R., Gelbard-Sagiv, H., Arieli, A., Fried, I., and Malach, R. (2007). Coupling between neuronal firing rate, gamma LFP, and BOLD fMRI is related to interneuronal correlations. Curr. Biol. *17*, 1275–1285. https://doi.org/10.1016/j.cub.2007.06.066.

8. Leopold, D.A., Murayama, Y., and Logothetis, N.K. (2003). Very slow activity fluctuations in monkey visual cortex: implications for functional brain imaging. Cereb. Cortex *13*, 422–433. https://doi.org/10.1093/cercor/13.4.422.

9. Kim, Y.J., van Rooij, S.J.H., Ely, T.D., Fani, N., Ressler, K.J., Jovanovic, T., and Stevens, J.S. (2019). Association between posttraumatic stress disorder severity and amygdala habituation to fearful stimuli. Depress. Anxiety *36*, 647–658. https://doi.org/10.1002/da.22928.

10. Admon, R., Lubin, G., Stern, O., Rosenberg, K., Sela, L., Ben-Ami, H., and Hendler, T.

(2009). Human vulnerability to stress depends on amygdala's predisposition and hippocampal plasticity. Proc. Natl. Acad. Sci. USA *106*, 14120–14125. https://doi.org/10.1073/pnas.0903183106.

11. Admon, R., Milad, M.R., and Hendler, T. (2013). A causal model of post-traumatic stress disorder: disentangling predisposed from acquired neural abnormalities. Trends Cogn. Sci. *17*, 337–347. https://doi.org/10.1016/j.tics.2013.05.005.

12. Stevens, J.S., Kim, Y.J., Galatzer-Levy, I.R., Reddy, R., Ely, T.D., Nemeroff, C.B., Hudak, L.A., Jovanovic, T., Rothbaum, B.O., and Ressler, K.J. (2017). Amygdala reactivity and anterior cingulate habituation predict posttraumatic stress disorder symptom maintenance after acute civilian trauma. Biol. Psychiatr. *81*, 1023–1029. https://doi.org/10.1016/j.biopsych.2016.11.015.

13. McTeague, L.M., Huemer, J., Carreon, D.M., Jiang, Y., Eickhoff, S.B., and Etkin, A. (2017). Identification of common neural circuit disruptions in cognitive control across psychiatric disorders. Am. J. Psychiatr. *174*, 676–685. https://doi.org/10.1176/appi.ajp.2017.16040400.

14. Collins, D.R., and Paré, D. (1999). Reciprocal changes in the firing probability of lateral and central medial amygdala neurons. J. Neurosci. *19*, 836–844. https://doi.org/10.1523/JNEUROSCI.19-02-00836.1999.

15. Rau, A.R., Chappell, A.M., Butler, T.R., Ariwodola, O.J., and Weiner, J.L. (2015). Increased basolateral amygdala pyramidal cell excitability may contribute to the anxiogenic phenotype induced by chronic early-life stress. J. Neurosci. *35*, 9730–9740. https://doi.org/10.1523/JNEUROSCI.0384-15.2015.

16. Hernandez, A., Burton, A.C., O'Donnell, P., Schoenbaum, G., and Roesch, M.R. (2015). Altered basolateral amygdala encoding in an animal model of schizophrenia. J. Neurosci. *35*, 6394–6400. https://doi.org/10.1523/JNEUROSCI.5096-14.2015.

17. Fenster, R.J., Lebois, L.A.M., Ressler, K.J., and Suh, J. (2018). Brain circuit dysfunction in post-traumatic stress disorder: from mouse to man. Nat. Rev. Neurosci. *19*, 535–551. https://doi.org/10.1038/s41583-018-0039-7.

18. Gavello, D., Calorio, C., Franchino, C., Cesano, F., Carabelli, V., Carbone, E., and Marcantoni, A. (2018). Early alterations of hippocampal neuronal firing induced by Abeta42. Cereb. Cortex *28*, 433–446. https://doi.org/10.1093/cercor/bhw377.

19. Keynan, J.N., Meir-Hasson, Y., Gilam, G., Cohen, A., Jackont, G., Kinreich, S., Ikar, L., Or-Borichev, A., Etkin, A., Gyurak, A., et al. (2016). Limbic activity modulation guided by functional magnetic resonance imaging–inspired Electroencephalography improves implicit emotion regulation. Biol. Psychiatr. *80*, 490–496. https://doi.org/10.1016/j.biopsych.2015.12.024.

20. Sigurdsson, T., and Duvarci, S. (2015). Hippocampal-prefrontal interactions in cognition, behavior and psychiatric disease. Front. Syst. Neurosci. *9*, 190. https://doi.org/10.3389/fnsys.2015.00190.

21. Meir-Hasson, Y., Kinreich, S., Podlipsky, I., Hendler, T., and Intrator, N. (2014). An EEG Finger-Print of fMRI deep regional activation. Neuroimage *102*, 128–141. https://doi.org/10.1016/j.neuroimage.2013.11.004.

22. Keynan, J.N., Cohen, A., Jackont, G., Green, N., Goldway, N., Davidov, A., Meir-Hasson, Y., Raz, G., Intrator, N., Fruchter, E., et al. (2019). Electrical fingerprint of the amygdala guides neurofeedback training for stress resilience. Nat. Hum. Behav. *3*, 63–73. https://doi.org/10.1038/s41562-018-0484-3.

23. Knott, J.R., Gibbs, F.A., and Henry, C.E. (1942). Fourier transforms of the electroencephalogram during sleep. J. Exp. Psychol. *31*, 465–477. https://doi.org/10.1037/h0058545.

24. Pitkänen, A., Pikkarainen, M., Nurminen, N., and Ylinen, A. (2000). Reciprocal connections between the amygdala and the hippocampal formation, perirhinal cortex, and postrhinal cortex in rat: a review. Ann. N. Y. Acad. Sci. *911*, 369–391. https://doi.org/10.1111/j.1749-6632.2000.tb06738.x.

25. Lendner, J.D., Helfrich, R.F., Mander, B.A., Romundstad, L., Lin, J.J., Walker, M.P., Larsson, P.G., and Knight, R.T. (2020). An electrophysiological marker of arousal level in humans. Elife *9*, e55092. https://doi.org/10.7554/eLife.55092.

26. Fahimi Hnazaee, M., Wittevrongel, B., Khachatryan, E., Libert, A., Carrette, E., Dauwe, I., Meurs, A., Boon, P., Van Roost, D., and Van Hulle, M.M. (2020). Localization of deep brain activity with scalp and subdural EEG. Neuroimage *223*, 117344. https://doi.org/10.1016/j.neuroimage.2020.117344.

27. Amunts, K., Kedo, O., Kindler, M., Pieperhoff, P., Mohlberg, H., Shah, N.J., Habel, U., Schneider, F., and Zilles, K. (2005). Cytoarchitectonic mapping of the human amygdala, hippocampal region and entorhinal cortex: intersubject variability and probability maps. Anat. Embryol. *210*, 343–352. https://doi.org/10.1007/s00429-005-0025-5.

28. Leutgeb, S., Leutgeb, J.K., Treves, A., Moser, M.-B., and Moser, E.I. (2004). Distinct ensemble codes in hippocampal areas CA3 and CA1. Science *305*, 1295–1298. https://doi.org/10.1126/science.1100265.

29. Sporns, O., and Zwi, J.D. (2004). The small world of the cerebral cortex. Neuroinformatics *2*, 145–162. https://doi.org/10.1385/NI:2:2:145.

30. Morgane, P.J., Galler, J.R., and Mokler, D.J. (2005). A review of systems and networks of the limbic forebrain/limbic midbrain. Prog. Neurobiol. *75*, 143–160. https://doi.org/10.1016/j.pneurobio.2005.01.001.

31. Stein, J.L., Wiedholz, L.M., Bassett, D.S., Weinberger, D.R., Zink, C.F., Mattay, V.S., and Meyer-Lindenberg, A. (2007). A validated network of effective amygdala connectivity. Neuroimage *36*, 736–745. https://doi.org/10.1016/j.neuroimage.2007.03.022.

32. Ranganath, C., Heller, A., Cohen, M.X., Brozinsky, C.J., and Rissman, J. (2005). Functional connectivity with the hippocampus during successful memory formation. Hippocampus *15*, 997–1005. https://doi.org/10.1002/hipo.20141.

33. Lalo, E., Thobois, S., Sharott, A., Polo, G., Mertens, P., Pogosyan, A., and Brown, P. (2008). Patterns of bidirectional communication between cortex and basal ganglia during movement in patients with Parkinson disease. J. Neurosci. *28*, 3008–3016. https://doi.org/10.1523/JNEUROSCI.5295-07.2008.

34. Gatev, P., Darbin, O., and Wichmann, T. (2006). Oscillations in the basal ganglia under normal conditions and in movement disorders. Mov. Disord. *21*, 1566–1577. https://doi.org/10.1002/mds.21033.

35. Nir, Y., Staba, R.J., Andrillon, T., Vyazovskiy, V.V., Cirelli, C., Fried, I., and Tononi, G. (2011). Regional slow waves and spindles in human sleep. Neuron *70*, 153–169. https://doi.org/10.1016/j.neuron.2011.02.043.

36. Whittingstall, K., and Logothetis, N.K. (2009). Frequency-band coupling in surface EEG reflects spiking activity in monkey visual cortex. Neuron *64*, 281–289. https://doi.org/10.1016/j.neuron.2009.08.016.

37. Iber, et al.. (2007). The AASM manual for the scoring of sleep and associated events: rules, terminology and technical specifications, *1* (Westchester, IL: American academy of sleep medicine).

38. Quiroga, R.Q., Nadasdy, Z., and Ben-Shaul, Y. (2004). Unsupervised spike detection and sorting with wavelets and superparamagnetic clustering. Neural Comput. *16*, 1661–1687. https://doi.org/10.1162/089976604774201631.

39. Stockwell, R.G., Mansinha, L., and Lowe, R.P. (1996). Localization of the complex spectrum: the S transform. IEEE Trans. Signal Process. *44*, 998–1001. https://doi.org/10.1109/78.492555.

40. de Curtis, M., and Avanzini, G. (2001). Interictal spikes in focal epileptogenesis. Prog. Neurobiol. *63*, 541–567. https://doi.org/10.1016/S0301-0082(00)00026-5.

41. Pearson, K. (1901). Principal components analysis. Lond. Edinb. Dublin Philos. Mag. J. Sci. *2*, 559–572.

42. Cattell, R.B. (1966). The scree test for the number of factors. Multivariate Behav. Res. *1*, 245–276. https://doi.org/10.1207/s15327906mbr0102_10.

STAR★METHODS

KEY RESOURCES TABLE

REAGENT or RESOURCE	SOURCE	IDENTIFIER
Software and algorithms		
MATLAB 2013a	MathWorks	https://www.mathworks.com/

RESOURCE AVAILABILITY

Lead contact

Further information and requests for resources and materials should be directed to and will be fulfilled by the lead contact, Talma Hendler (hendlert@gmail.com).

Materials availability

This study did not generate new materials.

Data and code availability

- All data reported in this paper will be shared by the lead contact upon request.
- This paper does not report original code.
- Any additional information required to reanalyze the data reported in this paper is available from the lead contact upon request.

EXPERIMENTAL MODEL AND SUBJECT DETAILS

Human participants

Thirteen patients with intractable epilepsy were implanted with depth electrodes to identify seizure foci for potential surgical intervention. Electrode location was based on clinical criteria. We examined six patients (2 males and 4 females, ages 32 $\pm$ 7.3) who had both amygdala and hippocampal units (of the 13 analyzed in Nir et al.[35]). All patients participated in a sleep study, which included episodes of wakefulness. Patients provided informed consent to participate in the study, which followed the guidelines of the Medical Institutional Review Board at UCLA.

METHOD DETAILS

All data analysis procedures were implemented using Matlab (Mathworks, USA). Data modeling was repeated several times per subject, brain region and state using five-fold cross-validation for performance evaluation, followed by complete data set modeling for additional analysis.

Data acquisition and spike sorting

8–12 depth electrodes were implanted in each patient. Each electrode terminated in eight 40-mm platinum-iridium microwires, from which extracellular signals were continuously recorded (referenced locally to a ninth non-insulated microwire) at a sampling rate of 28/30 kHz and bandpass-filtered between 1 and 6000 Hz. Scalp EEG (C3, C4, Fz and Pz) was continuously recorded at a sampling rate of 2 kHz, bandpass-filtered between 0.1 and 500 Hz, and re-referenced offline to the mean signal recorded from the earlobes. Recordings also included synchronized electro-oculogram, electromyogram and continuous video monitoring. The data was scored offline for sleep staging following established guidelines.[37]

Unit activity preprocessing

Spike sorting was performed offline using 'wave_clus'.[38] The number of isolated units from each subject and brain region are described in Table S1.

Most recorded units fired in low rates, ~90% from all recorded neurons in both wake and NREM sleep showed a firing rate $\leq$ 5 spikes/s and ~43% $\leq$ 1 spikes/s. Thus, spiking activity of all recorded neurons

in each brain region and time period used for training (wake and NREM sleep) were calculated in 5 s bins (number of spikes in each bin divided by the bin size in seconds). By doing so, we avoided transient fluctuations in firing activity and the relative sparseness of the recorded units. Applying linear regression is best suited for responses that are normally distributed, thus we visually inspected the distribution of the units firing rate and applied a transformation to best match a normal distribution. The chosen transformation was: $\sqrt[3]{x}$. For each unit we removed a small fraction of the time bins, in which its FR exceeded 5 times the standard deviation of its average activity. Those time bins were removed from all simultaneously recorded neurons. The firing rate was then averaged across neurons from both hemispheres and z-scored to have zero mean and standard deviation of one. The recorded units in both the amygdala and hippocampus did not form clustered activity (see Figure S2), which justified using the units' sample mean as a representative measure of regional activity.

To check for correlated activity within brain region we calculated the Pearson correlation coefficient between the firing rates (after transformation) of all the pairs of simultaneously recorded units.

EEG preprocessing

Four EEG channels were recorded per patient (C3, C4, Fz and Pz) at a 1 kHz sample rate, and were referenced to the mean of two electrodes located on the earlobes. EEG epochs in which the EEG amplitude of one of the channels exceeds 250 μV were considered artifacts and removed from further analysis (~1.5% of the 5 s bins were removed).

To calculate the power spectrum of the EEG signals we down-sampled the signal to 300 Hz and removed the mean amplitude of each 5 s time epoch (removing the DC component). Time frequency analysis was done using Stockwell transform[39] with a frequency resolution of 1 Hz. Stockwell transform provides frequency dependent resolution while maintaining a direct relationship with the Fourier spectrum. An example of the use of Stockwell transform in EEG can be found in Meir-Hasson et al.[21] The power in each 1 Hz bin was averaged per 5 s, and the frequency resolution was then reduced to 5 samples per time bin, according to the traditional division of EEG signal into frequency bands; delta (0-4 Hz), theta (4-8 Hz), alpha (8-16 Hz), beta (16-31 Hz), and low gamma (31-55 Hz) bands. Each EEG feature was z-scored to have a zero mean and standard deviation of one. This procedure produced an EEG feature matrix size N x 20, where N is the total number of time bins and 20 is the number of features (four scalp electrodes x five frequency bands per electrode). To validate rather the firing rate of frontal cortex units improve model performance we added their mean firing rate as an additional feature into the model. To validate whether arousal might improve the model performance we added four additional features, each is an estimate of the slope of the 1/f spectrum from each EEG channel in the frequency range 30-45 Hz[25] calculated from the spectrum of each 5 s bin using MATLAB polyfit function with n = 1, for a linear fit. FC mean firing rate and arousal features were also compared by themselves to the scalp EEG models.

Nir et al.[35] showed that neuronal spiking activity might be influenced from interictal epileptiform discharges, therefore we identified interictal activity at the target zone (amygdala or hippocampus) and excluded from further analysis any time bin in which such activity was identified. Interictal activity was detected by offline filtering the iEEG signal of the target area above 100 Hz and detecting events whose amplitude exceeded 5 SDs above the mean and whose duration was less than 70 μs.[40] For one subject (P396), all time points in the amygdala were kept, because it contained a large amount of interictal activity which did not lead to changes in firing rates.

As previously stated, linear regression is an additive model, and such a model usually benefit from features that are symmetrically distributed. Thus, we visually inspected the distribution of each feature and applied a transformation to best match a normal distribution. For the delta, theta and alpha bands we used a log transformation, for the beta band we used $1/x$ and for the gamma band we used $1/x^2$.

EEG feature extraction by principal component analysis

In most cases the EEG features were found to be highly correlated (see Figure S3A). In such cases, linear regression model coefficients can vary quite a bit, even with small perturbations of the data. We therefore performed principal component analysis (PCA) to reduce the excessive dimensionality of the input.

PCA[41] was performed separately for each of the patients' EEG feature matrix. To determine the number of principal components (PCs) to use, we examined each of the transformations scree plots (Eigen value vs. principal component number).[42] It revealed that the transition point from steep descent to a flat line occurs at the 6th PC for all subjects (Figure S3). Thus we chose to use the projection of the EEG feature matrix of the first 6 PCs as input to train the model (see Figures S3B and S3C). Using this number of PCs explained 92.85 $\pm$ 0.8% and 91.50 $\pm$ 1.36% of the variance over the 6 subjects in wakefulness and NREM sleep, respectively.

We used 8 and 9 first PCs respectively, when adding the frontal cortex mean neuron or the 1/f slope to the model, so that the explained variance is similar to that of the original model (which included only the frequency bands power).

QUANTIFICATION AND STATISTICAL ANALYSIS

Cross scales linear regression modeling

We used a linear regression to predict the firing rate (after transformation) from the EEG feature matrix (after PCA). For each brain region and patient, we calculated two models, one for wakefulness periods and the other for NREM sleep (REM sleep was not modeled because it occupied a relatively short period of our data (49.75 $\pm$ 12.20 min, mean $\pm$ sem). For each of the models we concatenated the relevant time bins, after discarding any irrelevant or noisy time bins. An examination of the Pearson correlations between single EEG features and target firing rates showed a very low and variable correlation across subjects. We therefore omitted this analysis from the report and used the multiple features jointly.

In order to obtain test predictions across the entire time frame we used five-fold cross validation. We split the data into five consecutive non-overlapping segments, training the model over 4/5 segments and testing for accuracy on the remaining segment. By choosing this validation process, and not randomly selecting the test data in between the train data, we were able to verify that the short timescale dependencies within the data would not facilitate model performance. Pearson correlation coefficient and root mean squared error (RMSE) between true and predicted FR were calculated as performance measures. Correlation values were compared to zero with a one-sided T test (α = 0.01, Bonferroni corrected for all the different models; n = 68). We also used an F-test on the regression model to assess a significance of the linear regression relationship between the FR and predictors (with a significance level of $p < 0.001$). The PCA over the features was calculated using the training data only, and the PCA calculated coefficients were used to transform the test data. Test correlation was defined as the Pearson correlation between all test periods concatenated to each other and their predicted values.

To check for the spatial specificity of the models, we used the model calculated for the amygdala/hippocampus to estimate the average unit activity of the hippocampus, amygdala and frontal cortex. This was performed in a similar 5-fold cross validation procedure as explained above. Depending on data availability, different frontal brain structures were used per subject to represent frontal cortex unit activity: P399 right and left supplementary motor area (12 and 11 units respectively), P402 right supplementary motor area (6 units), P405 right and left orbitofrontal cortex (7 and 2 units respectively), P406 right and left anterior cingulate cortex (4 and 3 units respectively), and P416 left orbitofrontal cortex (10 units).

Model assessments

To check for model stability, for each subject area and state we have calculated the pairwise Euclidean distance between each of the 5 different model coefficients from the 5-folds and averaged over it. After assessment of model accuracy in the cross validation setting and verifying similarity of model predictions across folds, the same multiple linear regression was applied to the entire time frame for further analyses (full model). Having found linear transformation models from the EEG PCA components to neural predictions, we could then compose the two transformations (PCA and regression model) into a single linear transform and report weights for the original EEG-band features.

To compare Pearson correlation between brain regions and states, correlations were subjected to Fisher's transform before applying any statistical test. In order to check the statistical properties of the per subject per region and state models performance, we created 60 different models each resulting from the different time shifts (5s–300s in 5s jumps) of the response vector (the firing rate) with the

un-shifted EEG feature matrix. We then visualized the calculated Fisher-transformed correlations between the firing rate and the predictions using boxplots for all shifted models. Since these are highly correlated and a strong trend is evident, these could not be used directly for testing. Nevertheless, corroborating evidence can be observed from the boxplots, such as the location of the un-shifted model away from the upper quartile, being the model with the highest correlation relative to the shifted ones, or being marked as an outlier. At the model level the assumption of independence can be more appropriate, so estimate and binomial confidence intervals for the proportion of models enjoying the property were constructed.